Experimental Animals
Exp. Anim. 69(1), 34–44, 2020

Original

Inhibition of long non-coding RNA metastasis-associated lung adenocarcinoma transcript 1 attenuates high glucose-induced cardiomyocyte apoptosis via regulation of miR-181a-5p

Yongxia CHENG[1–3], Jingchao LI[4], Chong WANG[1], Heran YANG[5], Ying WANG[6, 7], Tao ZHAN[1], Sufen GUO[1], Jun LIANG[3, 8], Yuxin BAI[1], Jianbo YU[1, 2] and Guibo LIU[6, 7]

[1]*Pathology Diagnosis Center, The First Clinical Medical School of Mudanjiang Medical College, No. 3 Tongxiang Street, Aimin District, Mudanjiang, Heilongjiang 157011, P.R.China*
[2]*Key Laboratory of Cancer Prevention and Treatment of Heilongjiang Province, Mudanjiang Medical College, No. 3 Tongxiang Street, Aimin District, Mudanjiang, Heilongjiang 157011, P.R.China*
[3]*Institute of Stem Cells, Mudanjiang Medical College, No. 3 Tongxiang Street, Aimin District, Mudanjiang, Heilongjiang 157011, P.R.China*
[4]*Department of Neurology, Hongqi Hospital of Mudanjiang Medical College, No. 3 Tongxiang Street, Aimin District, Mudanjiang, Heilongjiang 157011, P.R.China*
[5]*Department of Laboratory Medicine, Hongqi Hospital of Mudanjiang Medical College, No. 3 Tongxiang Street, Aimin District, Mudanjiang, Heilongjiang 157011, P.R.China*
[6]*Department of Anatomy, School of Basic Medical Sciences, Mudanjiang Medical College, No. 3 Tongxiang Street, Aimin District, Mudanjiang, Heilongjiang 157011, P.R.China*
[7]*Institute of Neural Tissue Engineering, Mudanjiang Medical College, No. 3 Tongxiang Street, Aimin District, Mudanjiang, Heilongjiang 157011, P.R.China*
[8]*Department of Histology and Embryology, School of Basic Medical Sciences, Mudanjiang Medical College, No. 3 Tongxiang Street, Aimin District, Mudanjiang, Heilongjiang 157011, P.R.China*

Abstract: Diabetic cardiomyopathy (DCM) is one of the cardiovascular complications of diabetes mellitus independent of hypertension, coronary disease, and other heart diseases. The development of DCM is multifactorial and hard to detect at an early stage. Long non-coding RNA metastasis-associated lung adenocarcinoma transcript 1 (*Malat1*) is emerging as a regulator of DCM, the underlying mechanism of its role in DCM has not been elaborated yet. In this study, we established a mouse DCM model via streptozocin injection as evidenced by cell hypertrophy and cell apoptosis of myocardial tissue, and found that *Malat1* expression was upregulated in the myocardium in DCM mice. Meanwhile, elevated expression of pro-apoptotic factors p53, p21, cleaved caspase 3, cleaved caspase 9 and BAX, and down-regulation of anti-apoptotic BCL-2 were observed in DCM myocardium. We further investigated the effect of *Malat1* on cardiomyocytes under high glucose condition by silencing *Malat1* with its specific short-hairpin RNA. Like *in vivo*, expression of *Malat1* in cardiomyocytes was notably raised, remarkable cell apoptosis and changes in apoptosis-related factors were also observed following high glucose treatment. Besides, we validated that *Malat1* acted as a sponge of miR-181a-5p. Inhibition of miR-181a-5p could, at least partially, abolish *Malat1* knockdown-induced alteration in cardiomyocytes. In addition, p53, a critical regulator of apoptosis, was validated to be a downstream target of miR-181a-5p. In summary, our findings reveal that *Malat1* knockdown attenuates high glucose-induced cardiomyocyte apoptosis via releasing miR-181a-5p, and this mechanism may provide us with new diagnosis target of DCM.

Key words: cardiomyocyte apoptosis, diabetic cardiomyopathy, metastasis-associated lung adenocarcinoma transcript 1, miR-181a-5p, p53

(Received 29 April 2019 / Accepted 1 July 2019 / Published online in J-STAGE 29 July 2019)
Corresponding author: G. Liu. e-mail: liuguibo_2017@163.com

Introduction

Diabetes mellitus (DM) is a metabolic disease featured by a high blood glucose level over a long period. DM is one of the largest global health emergencies of the 21st century owing to the extension of average life and increased obesity rate [5]. The prevalence of DM-related heart disease is in rapid and becomes a serious public health risk. The cardiovascular complications are the leading cause of diabetic patients, and studies show that the rate of heart failure is five times higher in diabetic women and two times higher in diabetic men [15, 36]. There are three major diabetic heart diseases: coronary artery disease (CAD), cardiac autonomic neuropathy (CAN), and diabetic cardiomyopathy (DCM) [29]. The terminology "diabetic cardiomyopathy" was first distinctly proposed in 1972 when heart failure was found in four diabetic patients [32]. DCM is specific cardiomyopathy in diabetic patients which is independent of coronary disease, hypertension, alcohol, and other structural heart diseases. It is characterized by left ventricular hypertrophy, interstitial fibrosis, cardiac microangiopathy and contractile dysfunction [25]. However, as the occurrence of DCM is multifactorial, there is no efficient and specific method for DCM diagnosis. Besides, DCM may remain asymptomatic for many years and accompany with other complications including obesity, hypertension, and vasculopathy, which makes the diagnosis of DCM even harder [19, 23]. Accordingly, exploring the underlying mechanism is of utmost importance for the diagnosis and treatment of DCM.

Long noncoding RNAs (lncRNAs) are defined as non-protein coding transcripts longer than 200 bp [13]. LncRNA metastasis-associated lung adenocarcinoma transcript 1 (*Malat1*), also known as noncoding nuclear-enriched abundant transcript 2 (*Neat2*), *Linc00047*, *Ncrn00047* and *Hcn*, is one of the first identified and most comprehensively studied lncRNAs [12]. *Malat1* was first discovered in non-small cell lung cancer and highly conserved among 33 mammalian species [14]. Since then, accumulating studies revealed its pivotal role in a variety of physiological processes. *Malat1* is involved in molecular modification such as alternative splicing, transcriptional regulation and post-transcriptional regulation [20, 35, 37]. *Malat1* is also implicated in various pathological processes including cancer development and progression, neurological disorders and, particularly, diabetes mellitus-related complications [2, 11, 30]. The expression of *Malat1* is significantly upregulated in rats with DM compared to control. Cardiomyocyte apoptosis is remarkably reduced after *Malat1* knockdown and left ventricular function is consequently improved in diabetic rats [39].

MicroRNAs (miRNAs) are another group of endogenous non-coding RNA that usually containing approximately 22 nucleotides [1]. MiRNAs participate in multiple pathways and processes owing to its low complementarity requirement between the sequences of miRNAs and their targets. MicroRNA miR-181a-5p was first found to be involved in carcinogenesis, and aberrant miR-181a-5p expression was responsible for abnormal cellular functions in cancers [18, 33]. A recent study revealed that miR-181a-5p was significantly downregulated in diabetic patients, diabetic rats, and high-glucose treated cardiomyocytes and that p53 and p21 acted as its target genes [31]. Besides, lncRNA could specifically bind to miR-181a-5p predicted on Starbase (http://starbase.sysu.edu.cn/index.php), which implies that *Malat1* may serve as a sponge of miR-181a-5p. Thus we hypothesize that *Malat1* is involved in DCM by regulating miR-181a-5p.

In this study, we examined the expression of *Malat1* and miR-181a-5p in mice with DCM. Then we investigated the effect of MLAT1 and miR-181a-5p on cardiomyocyte apoptosis. Furthermore, we validated the correlation between *Malat1* and miR-181a-5p.

Materials and Methods

Animal model establishment

Healthy C57BL/6J mice, 6–8 weeks old, were purchased from HKF (Shanghai, China). Mice were randomly divided into four groups: Control-4 weeks, DCM-4 weeks, Control-8 weeks, and DCM-8 weeks (n=6/group). Mice were intraperitoneally injected with 100 mg/kg streptozocin (STZ) (Aladdin, Shanghai, China) or the same volume normal saline (Dubang, Shenzhen, China) once a day for two days. A blood glucose level higher than 300 mg/dl demonstrated that the mouse diabetic model was successfully established. Mice were euthanized at week 4 and 8 following the STZ injection, and myocardial tissues were ultra-cryopreserved for subsequent detection. All animal experiments were carried out following the guideline for the care and use of laboratory animals and approved by Mudanjiang Medical College.

Cardiomyocyte isolation and viral infection

Cardiomyocytes were isolated as previously described [24]. In short, the heart of C57BL/6J mouse was carefully removed from thorax under a sterile environment and washed with PBS twice. Cardiac tissue was minced using curved scissors and digested with digestion buffer containing 1 mg/ml collagenase II, 1 mg/ml albumin and

25 μM $CaCl_2$. Digested tissues were then filtered with 140 μm screen mesh, cardiomyocytes were then cultured with serum-free Dulbecco's modified Eagle medium (DMEM) containing 0.2% albumin, 2 mM L-carnitine, 5 mM creatine, 5mM taurine, 0.1 μM insulin, 0.1 nM triiodothyronine and 10 mM 2,3-butanedione monoxime in a humidified incubator with 5% CO_2 at 37°C. The *Malat1* short hairpin RNA (sh*Malat1*) was inserted into lentivirus shuttle plasmid Tet-pLKO-puro between AgeI and EcoRI. Anti-miR-181a-5p sequence was also inserted into Tet-pLKO-puro. In order to investigate the effect of *Malat1* silencing on cardiomyocyte apoptosis, cardiomyocytes were infected with LV-sh*Malat1* (virus titer = 1×10^8 Tu/ml) and treated with 30 mM glucose for 48 h after infection. To further investigate the effect of miR-181a-5p inhibition on cardiomyocyte apoptosis, cardiomyocytes were co-infected with LV-sh*Malat1* and LV-anti-miR-181a-5p, and treated with 30 mM glucose for 48 h after infection. Sequences used in this study were as follow:

Malat1 shRNA: 5'-ccggcccGATTGAAGCTAGCAATCAAttcaagagaTTGATTGCTAGCTTCAATCttttt-3' (sense); NC shRNA: 5'-ccggcccTTCTCCGAACGTGTCACGTttcaagagaACGTGACACGTTCGGAGAAttttt-3' (sense).

Quantitative real-time PCR

Total RNAs of myocardial tissues and cardiomyocytes were extracted and reversely transcribed into cDNA using M-MLV reverse transcriptase (Tiangen, Beijing, China) following the manufacturer's manual. Quantitative real-time PCR was performed using SYBR Green mix (Solarbio, Beijing, China) and data were analyzed using the $2^{-\triangle\triangle CT}$ method. U6 snRNA was used as an internal control for miR-181a-5p and *Gapdh* was used as a control for *Malat1* and p53. Stem-loop RT primers for miRNAs and real-time PCR primers used in this study were as follows:

Mmu-miR-181a-5p specific stem-loop primer: 5'-GTTGGCTCTGGTGCAGGGTCCGAGGTATTCGCACCAGAGCCAACACTCAC-3';

U6 snRNA specific stem-loop primer: 5'-GTTGGCTCTGGTGCAGGGTCCGAGGTATTCGCACCAGAGCCAACAAAAATATGG-3';

Mmu-miR-181a-5p-Forward: 5'-CGGCAACATTCAACGCTGT-3'; Mmu-miR-181a-5p-Reverse: 5'-GTGCAGGGTCCGAGGTATTC-3';

U6 snRNA-Forward: 5'-CGCAAGGATGACACGCAAAT-3'; U6 snRNA-Reverse: 5'-GTGCAGGGTCCGAGGTATTC-3';

LncRNA *Malat1*-Forward: 5'-TTTGCGGGTGTTGTAGGTTT-3'; lncRNA *Malat1*-Reverse: 5'-ACAGGAGTGAGGCTTGTGGT-3';

P53-Forward: 5'-GGGCATGAACCGCCGACCTA-3'; p53-Reverse: 5'-GGCAGGCACAAACACGAACC-3'; GAPDH-Forward: 5'-TGTTCCTACCCCCAATGTGTCCGTC-3'; GAPDH-Reverse: 5'-CTGGTCCTCAGTGTAGCCCAAGATG-3'.

Western blot

Tissues and cells were lysed with RIPA lysis buffer containing 1 mM PMSF (Solarbio) and protein concentration was quantified using a BCA kit (Solarbio). Proteins were fractionated by sodium dodecyl sulfate-polyacrylamide gel electrophoresis (SDS-PAGE) and transferred to PVDF membranes (Millipore, Billerica, MA, USA). PVDF membranes were then blocked with 5% skim milk (Sangon Biotech, Shanghai, China) and incubated with one of the primary antibodies overnight at 4°C. After three-times PBS washing, PVDF membranes were incubated with certain secondary antibody for 60 min at 37°C. Primary antibodies used in this study were as follows: p53 antibody (1:2,000, Proteintech, Hangzhou, China), p21 antibody (1:1,000, Abcam, Cambridge, UK), cleaved caspase 3 antibody (1:1,000, CST, Framingham, MA, USA), cleaved caspase 9 antibody (1:1,000, CST), BCL-2 antibody (1:2,000, Proteintech), BAX antibody (1:5,000, Proteintech), and GAPDH antibody (1:10,000, Proteintech). HRP-conjugated goat anti-rabbit lgG (1:3,000, Solarbio) and HRP-conjugated goat anti-mouse lgG (1:3,000, Solarbio) were used as secondary antibodies.

Hematoxylin-eosin staining

Mouse myocardial tissues were embedded with paraffin and sliced into 5-μm sections, the paraffin sections were then deparaffinized and stained with hematoxylin and eosin successively. The morphological change of mouse myocardial tissues was photographed under a microscope (×400 magnification).

TdT mediated X-dUTP nicked labeling (TUNEL) assay

Cell apoptosis was detected via TUNEL staining. For mouse myocardial tissues, paraffin sections of 5 μm were deparaffinized and permeated with 0.1% Triton X-100. Afterward, sections were labeled with In Situ Cell Death Detection Kit (Roche, Basel, Switzerland), stained with hematoxylin and washed with gradient ethanol. The apoptosis of myocardial tissues was observed under a microscope (×400 magnification). For mouse cardiomyocytes, cell slides were permeated with 0.1% Triton X-100 and labeled with In Situ Cell Death Detection Kit at 37°C for 1 h. Then cell slides were stained with DAPI

 doi: 10.1538/expanim.19-0058

(Beyotime, Shanghai, China) for 5 min at room temperature and sealed with anti-fluorescence quenching reagent (Solarbio), typical pictures were captured under a microscope (×200 magnification).

Dual-luciferase assay

To investigate the correlation between lncRNA *Malat1* and miR-181a-5p, the wildtype and mutant type of *Malat1* fragments were inserted into pmirGLO (Promega, Madison, WI, USA) between Nhe I and Sal I, abbreviated as *Malat1*-WT and *Malat1*-MUT. 293T cells were co-transfected with *Malat1* plasmids and miR-181a-5p/NC mimics. To investigate the regulation of miR-181a-5p on p53, the wildtype and mutant type of p53 3'-UTR were inserted into pmirGLO between Nhe I and Sal I, abbreviated as p53-WT and p53-MUT. 293T cells were co-transfected with p53 3'-UTR and miR-181a-5p/Nonspecific control microRNA mimic, respectively. Cells were lysed and the binding activities were evaluated by firefly luciferase activity/renilla luciferase activity.

Statistical analysis

GraphPad Prism 7 was used to perform the data analysis. All results were presented as means ± SD and compared using Student's *t*-test (two groups) or One-way ANOVA (three or more groups). A P value<0.05 was considered as statistically significant.

Results

Mouse DCM model was successfully established

By hematoxylin-eosin staining, we found that myocardial fibers in control mice were arranged neatly, and

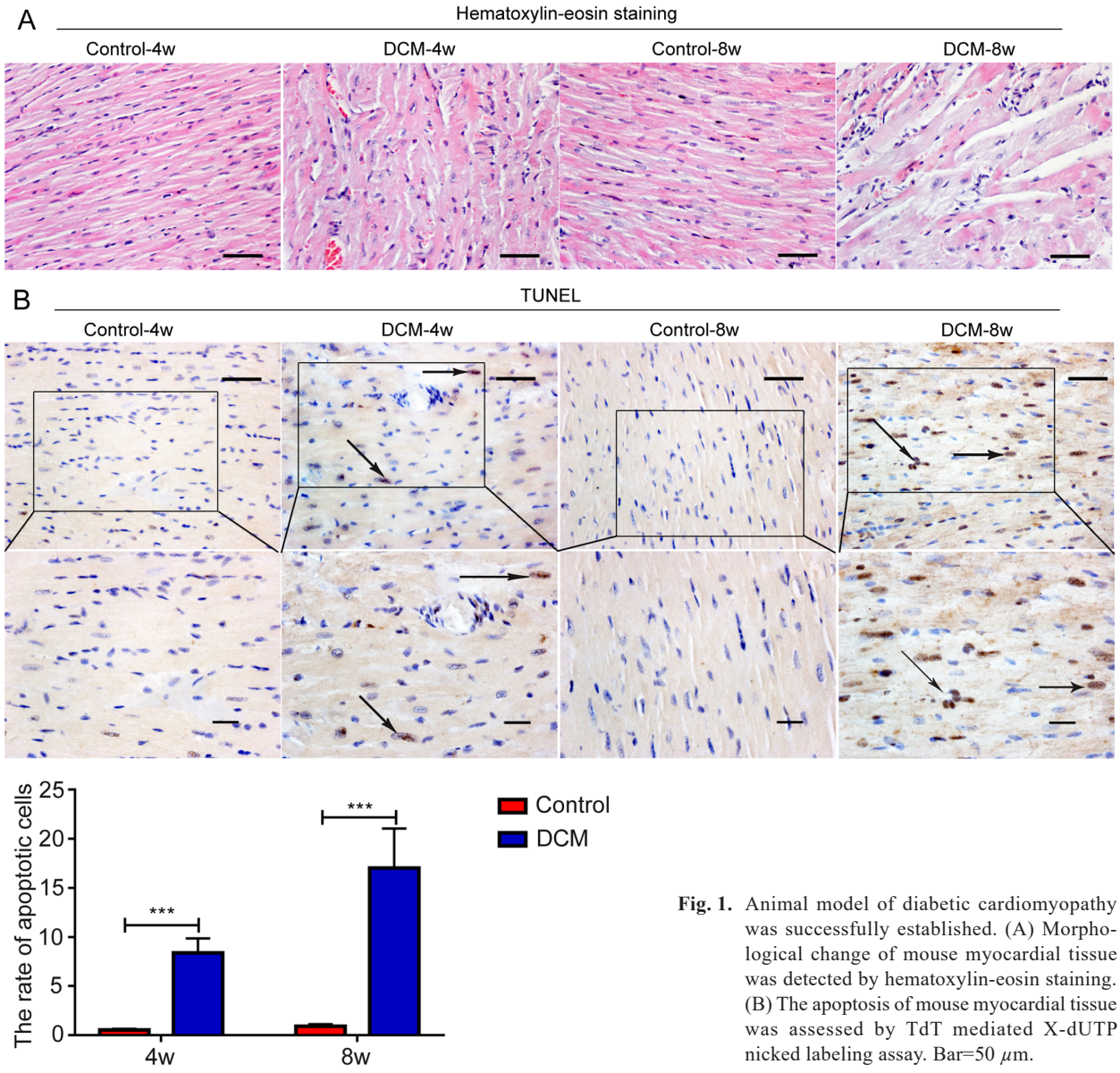

Fig. 1. Animal model of diabetic cardiomyopathy was successfully established. (A) Morphological change of mouse myocardial tissue was detected by hematoxylin-eosin staining. (B) The apoptosis of mouse myocardial tissue was assessed by TdT mediated X-dUTP nicked labeling assay. Bar=50 μm.

showed no cell swelling. Myocardial fibers of mice 4 weeks after STZ injection showed obvious disordered arrangement, cell hypertrophy and hyperchromatic nucleus. These characteristics were more notable at week 8, accompanied by cardiomyocyte necrosis and a large area of light staining (Fig. 1A). Then we detected the apoptosis in myocardial tissues using TUNEL assay. Cardiomyocytes in the control heart were arranged orderly and cell apoptosis was hardly detected. Four weeks post-STZ injection, cardiomyocytes were arranged disorderly, partial apoptotic cells were detected, which was more significant at week 8 (Fig. 1B). These results suggest that we successfully established the mouse diabetic cardiomyopathy model.

The expression of *Malat1*, miR-181a-5p and apoptosis-related factors in mice with DCM

We analyzed the expression changes of lncRNA *Malat1* and miR-181a-5p in mouse myocardial tissues by real-time PCR. *Malat1* was up-regulated at week 4 following STZ injection compared to control, which was even more significant at week 8. On the contrary, the RNA level of miR-181a-5p was remarkably decreased at week 4 after STZ treatment and the decrease was exacerbated at week 8 (Fig. 2A). Then we evaluated the expression of apoptosis-related factors by western blot. We found that the protein levels of p53, p21, cleaved caspase 3, cleaved caspase 9 and BAX were remarkably elevated at week 4 post-STZ injection in contrast with control, which were more significant at week 8. On the contrary, the expression of BCL-2 was significantly suppressed at week 8 after STZ injection in contrast with control (Fig. 2B). These results indicate that STZ injection induces cardiomyocyte apoptosis.

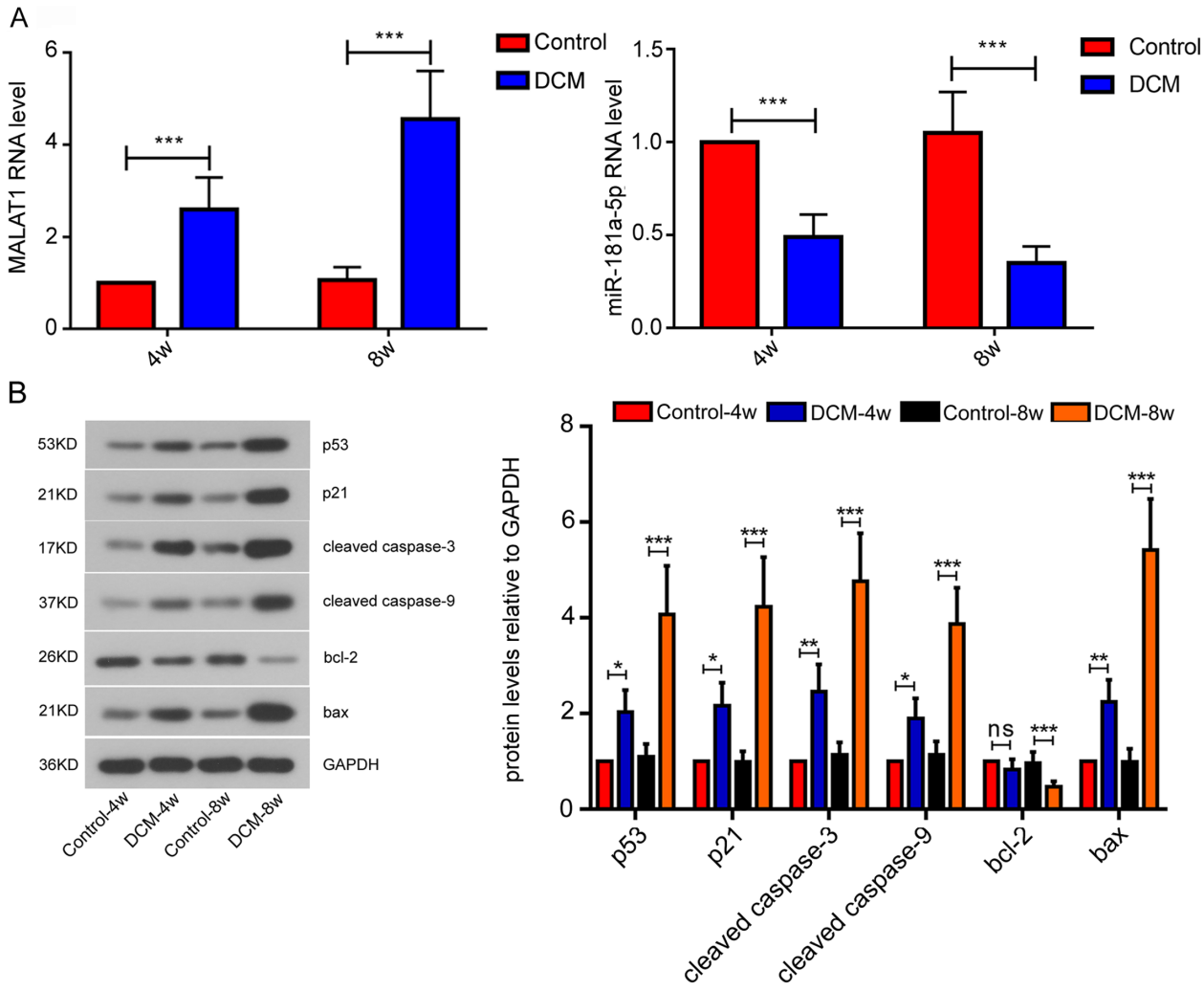

Fig. 2. Expression of long noncoding RNA *Malat1*, miR-181a-5p and apoptosis-related factors in mouse myocardial tissue. (A) The level of lncRNA *Malat1* and miR-181a-5p were measured by quantitative real-time PCR. (B) Protein levels of apoptosis-related factors were evaluated by western blot assay. All data were presented as mean ± SD. ns: not significant; **P*<0.05; ***P*<0.01; ****P*<0.001.

 doi: 10.1538/expanim.19-0058

Malat1 acts as a sponge of miR-181a-5p

Mouse cardiomyocyte treated with high glucose (HG) showed significant higher *Malat1* expression compared to mannitol group, and the expression of *Malat1* was successfully knocked down by sh*Malat1*. Like *in vivo*, the expression of miR-181a-5p showed the contrary trend to that of *Malat1*. The level of miR-181a-5p was downregulated following HG treatment but elevated after *Malat1* knockdown (Fig. 3A). These results inspired us to investigate the relationship between *Malat1* and miR-181a-5p. LncRNA *Malat1* could specifically bind to miR-181a-5p predicted on StarBase (http://starbase.sysu.edu.cn/index.php), and we validated their interaction by performing the dual-luciferase assay. The binding site of miR-181a-5p on *Malat1* was shown in Fig. 3B Cells co-transfected with *Malat1*-WT and miR-181a-5p mimics showed significantly weaker luciferase activity in contrast with that co-transfected with *Malat1*-WT and NC mimics. On the contrary, after *Malat1* mutation, no obvious difference of luciferase activity was observed between cells transfected with NC mimics and miR-181a-5p mimics (Fig. 3B).

Malat1 knockdown abrogates cardiomyocyte apoptosis induced by high glucose

We investigated the effect of *Malat1* on cardiomyocyte apoptosis via TUNEL assay. Obvious cardiomyocyte apoptosis was observed post the high glucose treatment. It was noteworthy that *Malat1* silencing abolished the apoptosis induced by high glucose (Fig. 4A). High glucose treatment significantly up-regulated the pro-apoptosis proteins including p53, p21, cleaved caspase 3, cleaved caspase 9 and BAX, yet inhibited the expression of BCL-2. *Malat1* silencing could alleviate the expression changes of these proteins induced by high glucose (Fig. 4B). These results indicate that *Malat1* silencing can suppress cardiomyocyte apoptosis.

The effect of miR-181a-5p on cardiomyocyte apoptosis

Owing to the interaction between *Malat1* and miR-181a-5p, we further investigated the effect of miR-181a-5p on cardiomyocyte apoptosis. Like we previously described, *Malat1* knockdown abrogated the high glucose-induced cardiomyocyte apoptosis. Then we sup-

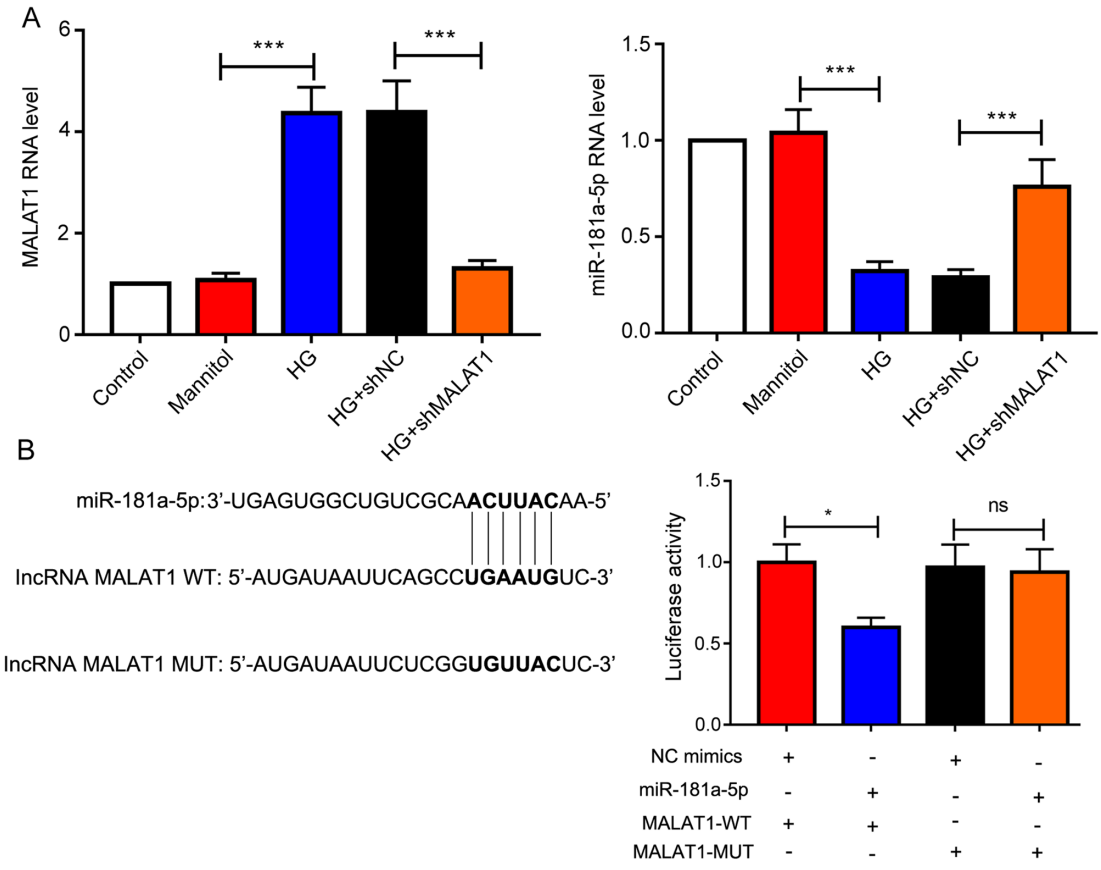

Fig. 3. Long noncoding RNA *Malat1* acts as a sponge of miR-181a-5p. (A) The levels of lncRNA *Malat1* and miR-181a-5p in mouse cardiomyocytes after *Malat1* silencing were measured by quantitative real-time PCR. (B) The specific binding site of miR-181a-5p on *Malat1* was shown, and the correlation between *Malat1* and miR-181a-5p was analyzed by dual-luciferase assay, ns: not significant; **P*<0.05; *** *P*<0.001.

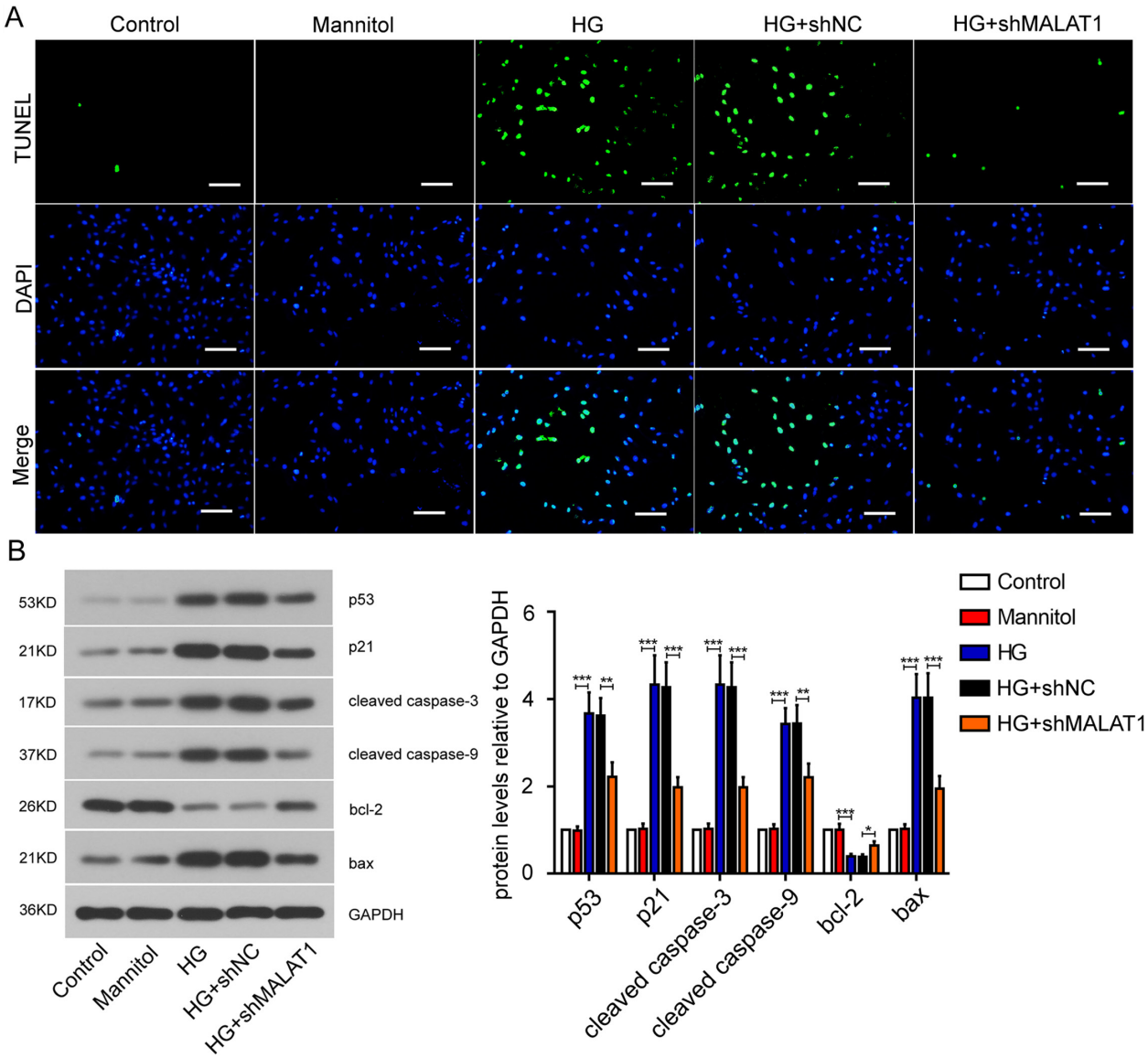

Fig. 4. Effect of *Malat1* silencing on mouse cardiomyocyte apoptosis. (A) Apoptosis of mouse cardiomyocytes after *Malat1* silencing was detected by TdT mediated X-dUTP nicked labeling assay (Bar=100 μm). (B) Expression of apoptosis-related factors after *Malat1* silencing was measured by western blot assay. All data were presented as mean ± SD. **P*<0.05; ***P*<0.01; ****P*<0.001.

pressed the miR-181a-5p expression with anti-miR-181a-5p viral particles, and apoptotic cells re-appeared (Fig. 5A). *Malat1* silencing down-regulated the expression of p53, p21, cleaved caspase 3, cleaved caspase 9 and BAX, but elevated the protein level of BCL-2. All these expression changes were remarkably reversed after miR-181a-5p inhibition (Fig. 5B). These results suggest that miR-181a-5p is involved in *Malat1*-mediated cardiomyocyte apoptosis.

P53 is a downstream target of miR-181a-5p

The binding site of miR-181a-5p and p53 was shown in Fig. 6A Cells co-transfected with p53-WT and miR-181a-5p mimics showed notably weaker luciferase activity compared to that co-transfected with p53-WT and NC mimics. There was no difference of luciferase activity between cells co-transfected with p53-MUT + NC mimics and that co-transfected with p53-MUT + miR-181a-5p mimics (Fig. 6A). Furthermore, the mRNA level of p53 was remarkably elevated after miR-181a-5p inhibition, demonstrating that p53 is a downstream target of miR-181a-5p.

Discussion

Cardiovascular-related complications are responsible for approximately 65% of diabetic death [29]. Among which DCM leads to diastolic dysfunction and further systolic dysfunction, and eventually greatly increases the risk of heart failure [10]. Myocardial fibrosis and

 doi: 10.1538/expanim.19-0058

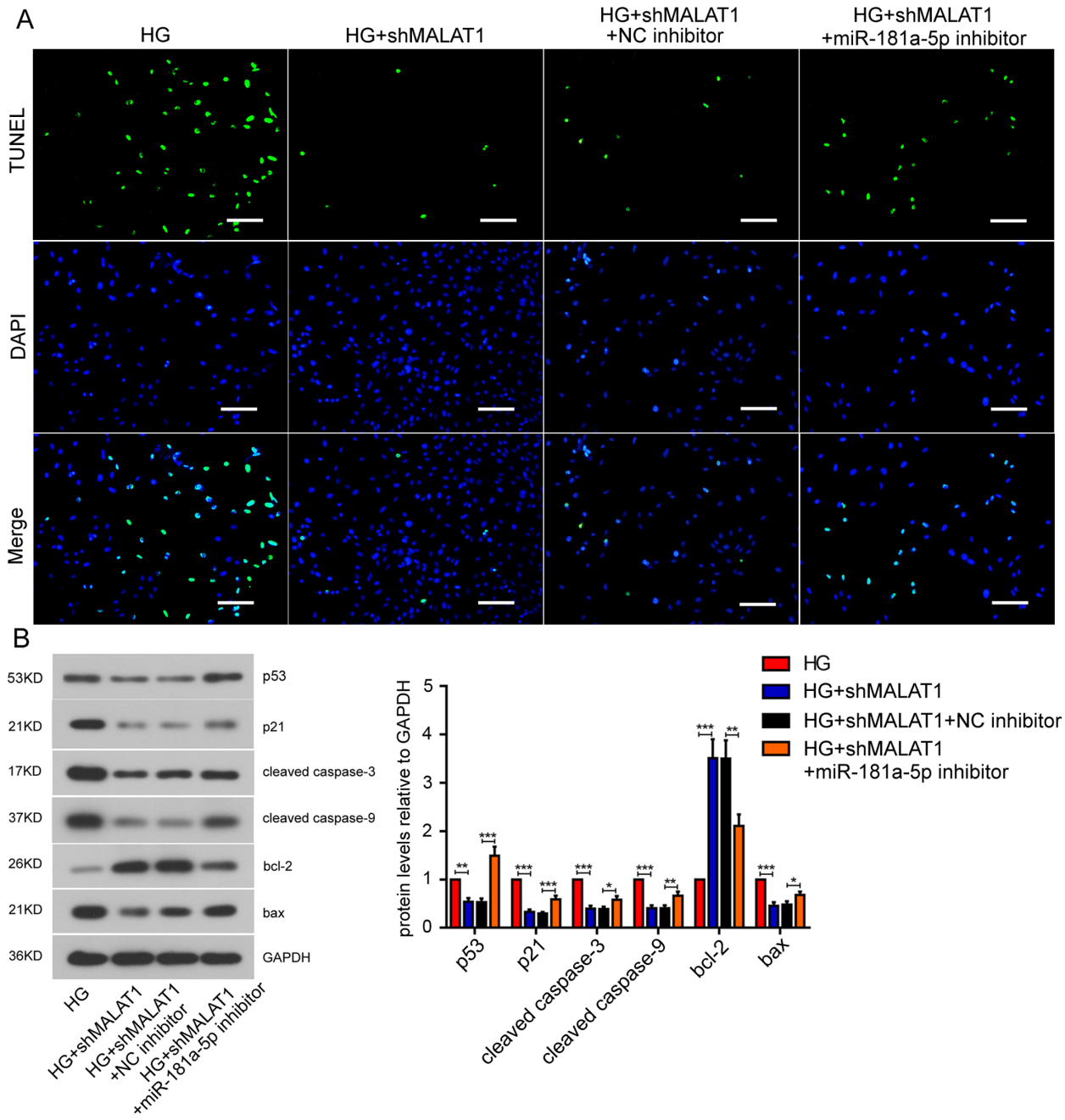

Fig. 5. Effect of miR-181a-5p on mouse cardiomyocytes apoptosis. (A) Apoptosis of mouse cardiomyocytes after miR-181a-5p inhibition was assessed by TdT mediated X-dUTP nicked labeling assay (Bar=100 μm). (B) Protein levels of apoptosis-related factors after miR-181a-5p inhibition were detected by western blot assay. All data were presented as mean ± SD. **P*<0.05; ***P*<0.01; ****P*<0.001.

hypertrophy, as well as cardiomyocyte apoptosis, are vital contributors in the onset and progression of DCM [9]. In this study, we established a mouse DCM model via intraperitoneal injection of STZ according to a previous study [34]. Clear hypertrophy of myocardial fibers and myocardial necrosis were detectable at week 8 following STZ injection. TUNEL assay further showed that STZ treatment led to substantial cardiomyocyte apoptosis. Taken all these together, we built an appropriate model for investigations of DCM.

The major pathological characteristics of DM patients include hyperglycemia, hyperlipidemia, and inflammation, among which hyperglycemia is widely believed to be the leading cause of DCM pathogenesis [28]. Sustained hyperglycemia leads to a variety of metabolic changes in cardiomyocytes including oxidative stress through the development of reactive oxygen species (ROS), which could further induce the apoptosis and DNA damage of cardiomyocytes [3, 8]. Hyperglycemia-induced cardiomyocytes apoptosis is regulated by

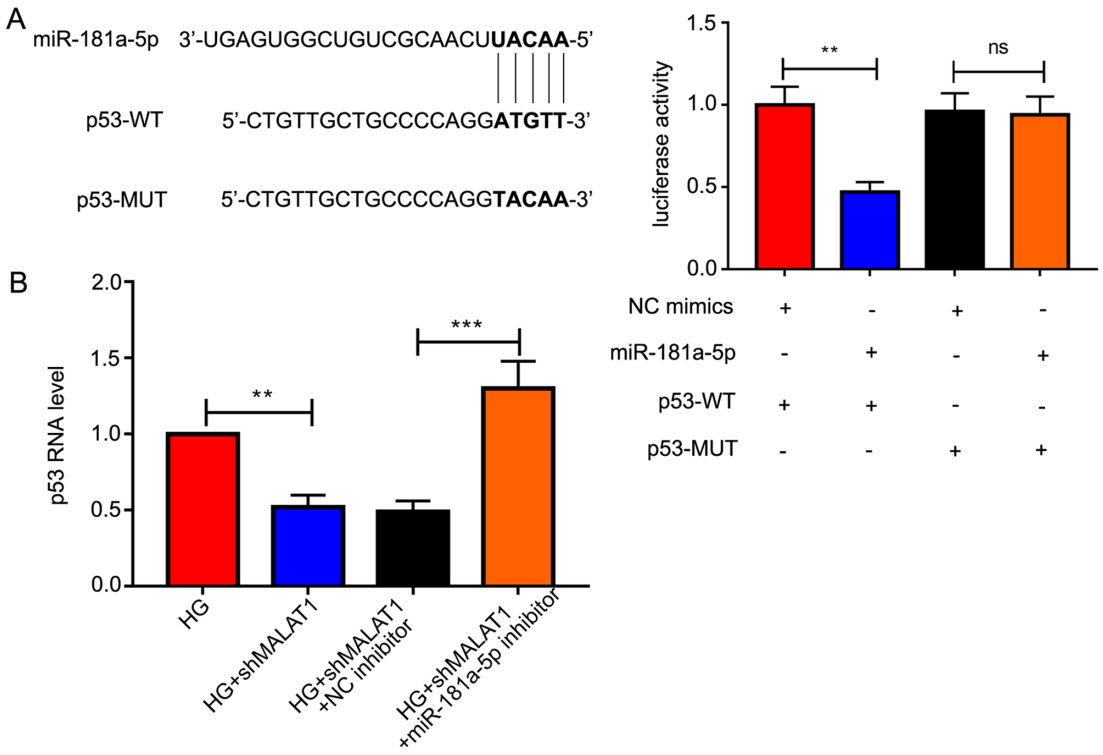

Fig. 6. P53 is a downstream target gene of miR-181a-5p. (A) The specific binding site of miR-181a-5p on p53 was displayed, and the correlation between miR-181a-5p and p53 was assessed by dual-luciferase assay. (B) The mRNA level of p53 after miR-181a-5p inhibition was measured by quantitative real-time PCR. All data were presented as mean ± SD. ns: not significant; ***P*<0.01; ****P*<0.001.

the mitochondrial apoptotic pathway, as evidenced by the release of cytochrome c and activation of caspase 3 [3]. Furthermore, p53, a well-known tumor suppressor, is involved in the development of oxidative damage-induced cardiomyopathy through regulating p21 [26]. P53 also interacts with p21 to inhibit cell proliferation and induce cell apoptosis via activating BAX [16]. In particular, the expression of p53 is significantly up-regulated in diabetic mice and leads to cardiac dysfunction, whereas cardiac impairment is abolished in p53 knock-out mice [27]. In this study, the elevated expression of p53, p21, cleaved caspase 3, cleaved caspase 9, and pro-apoptotic BAX, and down-regulation of anti-apoptotic BCL-2 were detected in the myocardium of STZ-induced DCM mice, indicating that mitochondrial apoptotic pathway mediated apoptosis occurred in diabetic myocardial tissue. Similar cell apoptosis was also observed in high glucose-treated cardiomyocytes, indicating that hyperglycemia could result in cardiomyocyte apoptosis *in vitro*.

LncRNAs are involved in various physiological processes via binding to DNA/RNA/protein or changing the localization/affinity of protein [6]. They also regulate gene expression via decoying specific microRNAs. Increasing evidence indicates that abnormal expression of lncRNAs is implicated in cardiovascular complications of diabetes [7]. *Malat1*, highly conserved among various mammals, is emerging as a regulator of DCM. For instance, *Malat1* is notably up-regulated in myocardial tissue of diabetic rats. Knockdown of *Malat1* significantly improved the left ventricular end-diastolic diameter (LVEDD) and left ventricular end-systolic diameter (LVESD), indicating that *Malat1* silencing could abrogate the cardiac impairment of diabetic rats [38]. Besides, cardiomyocyte apoptosis was reduced and cardiac function was improved in diabetic rats after *Malat1* knockdown [39]. Our results, in accord with previous studies, demonstrated that *Malat1* was up-regulated in DCM mice and high glucose-treated cardiomyocytes. Knockdown of *Malat1* via sh*Malat1* significantly alleviated apoptosis induced by high glucose as evidenced by expression changes of apoptosis-related proteins. MiR-181a-5p was found to be involved in regulating apoptosis of endothelial cells [4]. MiR-181a-5p also promotes invasion of hepatocellular carcinoma by p53 signaling pathway [21]. Our study first validated the interaction between *Malat1* and miR-181a-5p, whose expression levels were opposite in both diabetic myocardial tissues and high glucose-treated cardiomyocytes. Inhibition of miR-181a-5p could partially reverse the anti-apoptotic effect of sh*Malat1*. In particular, miR-181a-5p is down-regulated in DCM rats developed by high-fat diet and

 doi: 10.1538/expanim.19-0058

low-dose STZ, and decreased miR-181a-5p promotes cell apoptosis via regulating the p53-p21 pathway [31, 40]. Increasing evidence revealed that aberrant microRNA expression is associated with diabetic cardiovascular complications. For instance, cardiomyocyte hypertrophy induced by diabetes showed close relationship with down-regulation of miR-150, miR-133a and miR-30c, among which elevated miR-30c expression could alleviate the cardiomyocyte hypertrophy [22]. MiR-30d, miR-133a, miR-206, and miR-1 are involved in diabetes-induced cardiomyocyte apoptosis as well as mitochondrial dysfunction[22]. For clinical application, a previous clinical study showed that the expression of seven microRNAs is remarkably up-regulated in diabetic patients in contrast with pre-diabetes patients and susceptible individuals [17]. DCM is hard to detect at the early stage of the disease, thus the serum levels of microRNAs could act as a sensitive and efficient indicator for the cardiovascular complication of diabetes [17].

In conclusion, our study demonstrates that *Malat1* promotes cardiomyocyte apoptosis by preventing miR-181a-5p from binding to p53. *Malat1*-miR-181a-5p-p53 might serve as a therapeutic target for DCM.

Conflict of Interest

None.

Acknowledgments

This study was supported by grants from the Natural Science Foundation of Heilongjiang Province (No. H2018069), the Scientific Research Projects for Heilongjiang Provincial Universities (No. 2017-KYYWF-MY-0678 and 2018-KYYWFMY-0078), the Scientific Research Project of Health and Family Planning Commission of Heilongjiang Province (No. 2017-313), and the National Natural Science Foundation of China (No. 81870977).

References

1. Bartel, D.P. 2004. MicroRNAs: genomics, biogenesis, mechanism, and function. *Cell* 116: 281–297. [Medline] [CrossRef]
2. Bernard, D., Prasanth, K.V., Tripathi, V., Colasse, S., Nakamura, T., Xuan, Z., Zhang, M.Q., Sedel, F., Jourdren, L., Coulpier, F., Triller, A., Spector, D.L. and Bessis, A. 2010. A long nuclear-retained non-coding RNA regulates synaptogenesis by modulating gene expression. *EMBO J.* 29: 3082–3093. [Medline] [CrossRef]
3. Cai, L., Li, W., Wang, G., Guo, L., Jiang, Y. and Kang, Y.J. 2002. Hyperglycemia-induced apoptosis in mouse myocardium: mitochondrial cytochrome C-mediated caspase-3 activation pathway. *Diabetes* 51: 1938–1948. [Medline] [CrossRef]
4. Carmona, A., Guerrero, F., Buendia, P., Obrero, T., Aljama, P. and Carracedo, J. 2017. Microvesicles Derived from Indoxyl Sulfate Treated Endothelial Cells Induce Endothelial Progenitor Cells Dysfunction. *Front. Physiol.* 8: 666. [Medline] [CrossRef]
5. Chiang, J.L., Kirkman, M.S., Laffel, L.M., Peters, A.L., Type 1 Diabetes Sourcebook Authors. 2014. Type 1 diabetes through the life span: a position statement of the American Diabetes Association. *Diabetes Care* 37: 2034–2054. [Medline] [CrossRef]
6. Chien, H.Y., Chen, C.Y., Chiu, Y.H., Lin, Y.C. and Li, W.C. 2016. Differential microRNA Profiles Predict Diabetic Nephropathy Progression in Taiwan. *Int. J. Med. Sci.* 13: 457–465. [Medline] [CrossRef]
7. Das, A., Samidurai, A. and Salloum, F.N. 2018. Deciphering Non-coding RNAs in Cardiovascular Health and Disease. *Front. Cardiovasc. Med.* 5: 73. [Medline] [CrossRef]
8. Du, X., Matsumura, T., Edelstein, D., Rossetti, L., Zsengellér, Z., Szabó, C. and Brownlee, M. 2003. Inhibition of GAPDH activity by poly(ADP-ribose) polymerase activates three major pathways of hyperglycemic damage in endothelial cells. *J. Clin. Invest.* 112: 1049–1057. [Medline] [CrossRef]
9. Falcão-Pires, I. and Leite-Moreira, A.F. 2012. Diabetic cardiomyopathy: understanding the molecular and cellular basis to progress in diagnosis and treatment. *Heart Fail. Rev.* 17: 325–344. [Medline] [CrossRef]
10. Gilca, G.E., Stefanescu, G., Badulescu, O., Tanase, D.M., Bararu, I. and Ciocoiu, M. 2017. Diabetic Cardiomyopathy: Current Approach and Potential Diagnostic and Therapeutic Targets. *J. Diabetes Res.* 2017: 1310265. [Medline] [CrossRef]
11. Gutschner, T., Hämmerle, M. and Diederichs, S. 2013. MALAT1 -- a paradigm for long noncoding RNA function in cancer. *J. Mol. Med. (Berl.)* 91: 791–801. [Medline] [CrossRef]
12. Hutchinson, J.N., Ensminger, A.W., Clemson, C.M., Lynch, C.R., Lawrence, J.B. and Chess, A. 2007. A screen for nuclear transcripts identifies two linked noncoding RNAs associated with SC35 splicing domains. *BMC Genomics* 8: 39. [Medline] [CrossRef]
13. Iyer, M.K., Niknafs, Y.S., Malik, R., Singhal, U., Sahu, A., Hosono, Y., Barrette, T.R., Prensner, J.R., Evans, J.R., Zhao, S., Poliakov, A., Cao, X., Dhanasekaran, S.M., Wu, Y.M., Robinson, D.R., Beer, D.G., Feng, F.Y., Iyer, H.K. and Chinnaiyan, A.M. 2015. The landscape of long noncoding RNAs in the human transcriptome. *Nat. Genet.* 47: 199–208. [Medline] [CrossRef]
14. Ji, P., Diederichs, S., Wang, W., Böing, S., Metzger, R., Schneider, P.M., Tidow, N., Brandt, B., Buerger, H., Bulk, E., Thomas, M., Berdel, W.E., Serve, H. and Müller-Tidow, C. 2003. MALAT-1, a novel noncoding RNA, and thymosin beta4 predict metastasis and survival in early-stage non-small cell lung cancer. *Oncogene* 22: 8031–8041. [Medline] [CrossRef]
15. Kannel, W.B. and McGee, D.L. 1979. Diabetes and cardiovascular disease. The Framingham study. *JAMA* 241: 2035–2038. [Medline] [CrossRef]
16. Kim, E.M., Jung, C.H., Kim, J., Hwang, S.G., Park, J.K. and Um, H.D. 2017. The p53/p21 Complex Regulates Cancer Cell Invasion and Apoptosis by Targeting Bcl-2 Family Proteins. *Cancer Res.* 77: 3092–3100. [Medline] [CrossRef]
17. Kong, L., Zhu, J., Han, W., Jiang, X., Xu, M., Zhao, Y., Dong, Q., Pang, Z., Guan, Q., Gao, L., Zhao, J. and Zhao, L. 2011. Significance of serum microRNAs in pre-diabetes and newly diagnosed type 2 diabetes: a clinical study. *Acta Diabetol.* 48: 61–69. [Medline] [CrossRef]
18. Lashine, Y.A., Seoudi, A.M., Salah, S. and Abdelaziz, A.I. 2011. Expression signature of microRNA-181-a reveals its crucial role in the pathogenesis of paediatric systemic lupus erythematosus. *Clin. Exp. Rheumatol.* 29: 351–357. [Medline]
19. Lee, W.S. and Kim, J. 2017. Diabetic cardiomyopathy: where

we are and where we are going. *Korean J. Intern. Med. (Korean. Assoc. Intern. Med.)* 32: 404–421. [Medline]
20. Leucci, E., Patella, F., Waage, J., Holmstrøm, K., Lindow, M., Porse, B., Kauppinen, S. and Lund, A.H. 2013. microRNA-9 targets the long non-coding RNA MALAT1 for degradation in the nucleus. *Sci. Rep.* 3: 2535. [Medline] [CrossRef]
21. Liu, S., Yao, X., Zhang, D., Sheng, J., Wen, X., Wang, Q., Chen, G., Li, Z., Du, Z. and Zhang, X. 2018. Analysis of Transcription Factor-Related Regulatory Networks Based on Bioinformatics Analysis and Validation in Hepatocellular Carcinoma. *BioMed Res. Int.* 2018: 1431396. [Medline] [CrossRef]
22. Liu, X. and Liu, S. 2017. Role of microRNAs in the pathogenesis of diabetic cardiomyopathy. *Biomed. Rep.* 6: 140–145. [Medline] [CrossRef]
23. Lorenzo-Almorós, A., Tuñón, J., Orejas, M., Cortés, M., Egido, J. and Lorenzo, Ó. 2017. Diagnostic approaches for diabetic cardiomyopathy. *Cardiovasc. Diabetol.* 16: 28. [Medline] [CrossRef]
24. Luo, J., Hill, B.G., Gu, Y., Cai, J., Srivastava, S., Bhatnagar, A. and Prabhu, S.D. 2007. Mechanisms of acrolein-induced myocardial dysfunction: implications for environmental and endogenous aldehyde exposure. *Am. J. Physiol. Heart Circ. Physiol.* 293: H3673–H3684. [Medline] [CrossRef]
25. Miki, T., Yuda, S., Kouzu, H. and Miura, T. 2013. Diabetic cardiomyopathy: pathophysiology and clinical features. *Heart Fail. Rev.* 18: 149–166. [Medline] [CrossRef]
26. Mönkemann, H., De Vriese, A.S., Blom, H.J., Kluijtmans, L.A., Heil, S.G., Schild, H.H. and Golubnitschaja, O. 2002. Early molecular events in the development of the diabetic cardiomyopathy. *Amino Acids* 23: 331–336. [Medline] [CrossRef]
27. Nakamura, H., Matoba, S., Iwai-Kanai, E., Kimata, M., Hoshino, A., Nakaoka, M., Katamura, M., Okawa, Y., Ariyoshi, M., Mita, Y., Ikeda, K., Okigaki, M., Adachi, S., Tanaka, H., Takamatsu, T. and Matsubara, H. 2012. p53 promotes cardiac dysfunction in diabetic mellitus caused by excessive mitochondrial respiration-mediated reactive oxygen species generation and lipid accumulation. *Circ Heart Fail* 5: 106–115. [Medline] [CrossRef]
28. Nishikawa, T., Edelstein, D., Du, X.L., Yamagishi, S., Matsumura, T., Kaneda, Y., Yorek, M.A., Beebe, D., Oates, P.J., Hammes, H.P., Giardino, I. and Brownlee, M. 2000. Normalizing mitochondrial superoxide production blocks three pathways of hyperglycaemic damage. *Nature* 404: 787–790. [Medline] [CrossRef]
29. Pappachan, J.M., Varughese, G.I., Sriraman, R. and Arunagirinathan, G. 2013. Diabetic cardiomyopathy: Pathophysiology, diagnostic evaluation and management. *World J. Diabetes* 4: 177–189. [Medline] [CrossRef]
30. Puthanveetil, P., Chen, S., Feng, B., Gautam, A. and Chakrabarti, S. 2015. Long non-coding RNA MALAT1 regulates hyperglycaemia induced inflammatory process in the endothelial cells. *J. Cell. Mol. Med.* 19: 1418–1425. [Medline] [CrossRef]
31. Raut, S.K., Singh, G.B., Rastogi, B., Saikia, U.N., Mittal, A., Dogra, N., Singh, S., Prasad, R. and Khullar, M. 2016. miR-30c and miR-181a synergistically modulate p53-p21 pathway in diabetes induced cardiac hypertrophy. *Mol. Cell. Biochem.* 417: 191–203. [Medline] [CrossRef]
32. Rubler, S., Dlugash, J., Yuceoglu, Y.Z., Kumral, T., Branwood, A.W. and Grishman, A. 1972. New type of cardiomyopathy associated with diabetic glomerulosclerosis. *Am. J. Cardiol.* 30: 595–602. [Medline] [CrossRef]
33. Seoudi, A.M., Lashine, Y.A. and Abdelaziz, A.I. 2012. MicroRNA-181a - a tale of discrepancies. *Expert Rev. Mol. Med.* 14: e5. [Medline] [CrossRef]
34. Towner, R.A., Smith, N., Saunders, D., Carrizales, J., Lupu, F., Silasi-Mansat, R., Ehrenshaft, M. and Mason, R.P. 2015. In vivo targeted molecular magnetic resonance imaging of free radicals in diabetic cardiomyopathy within mice. *Free Radic. Res.* 49: 1140–1146. [Medline] [CrossRef]
35. Tripathi, V., Ellis, J.D., Shen, Z., Song, D.Y., Pan, Q., Watt, A.T., Freier, S.M., Bennett, C.F., Sharma, A., Bubulya, P.A., Blencowe, B.J., Prasanth, S.G. and Prasanth, K.V. 2010. The nuclear-retained noncoding RNA MALAT1 regulates alternative splicing by modulating SR splicing factor phosphorylation. *Mol. Cell* 39: 925–938. [Medline] [CrossRef]
36. Wang, Z.V. and Hill, J.A. 2015. Diabetic cardiomyopathy: catabolism driving metabolism. *Circulation* 131: 771–773. [Medline] [CrossRef]
37. West, J.A., Davis, C.P., Sunwoo, H., Simon, M.D., Sadreyev, R.I., Wang, P.I., Tolstorukov, M.Y. and Kingston, R.E. 2014. The long noncoding RNAs NEAT1 and MALAT1 bind active chromatin sites. *Mol. Cell* 55: 791–802. [Medline] [CrossRef]
38. Zhang, M., Gu, H., Chen, J. and Zhou, X. 2016. Involvement of long noncoding RNA MALAT1 in the pathogenesis of diabetic cardiomyopathy. *Int. J. Cardiol.* 202: 753–755. [Medline] [CrossRef]
39. Zhang, M., Gu, H., Xu, W. and Zhou, X. 2016. Down-regulation of lncRNA MALAT1 reduces cardiomyocyte apoptosis and improves left ventricular function in diabetic rats. *Int. J. Cardiol.* 203: 214–216. [Medline] [CrossRef]
40. Zhu, D.X., Zhu, W., Fang, C., Fan, L., Zou, Z.J., Wang, Y.H., Liu, P., Hong, M., Miao, K.R., Liu, P., Xu, W. and Li, J.Y. 2012. miR-181a/b significantly enhances drug sensitivity in chronic lymphocytic leukemia cells via targeting multiple anti-apoptosis genes. *Carcinogenesis* 33: 1294–1301. [Medline] [CrossRef]